BMC Ophthalmology

RESEARCH

Open Access

In-vivo sclera thickness measurements in experimental myopia of guinea pigs

Ruiheng Zhang[1,2,3†], Chuyao Yu[1,2,3†], Li Dong[1,2,3], Yitong Li[1,2,3], Xuhan Shi[1,2,3], Haotian Wu[1,2,3], Wenda Zhou[1,2,3], Heyan Li[1,2,3] and Wenbin Wei[1,2,3*]

Abstract

The sclera is the target organ of axial elongation during myopia onset and progression. Visualizing the sclera in-vivo is important for monitoring the dynamic changes of the sclera remodeling in experimental myopia. In the present study, three-week-old tricolor guinea pigs were subjected to negative controls ($n=8$), monocular negative lens-induced myopia (LIM, $n=10$), or combining monocular LIM and intravitreally mTORC1 agonist (MHY1485, 4 µg) injection for inducing high myopia (LIM + MHY1485 group, $n=10$) for four weeks. Serial biometric measurements were performed to monitor experimental myopia onset and progression. Swept-source optical coherence tomography (SS-OCT) was performed to measure sclera thickness at the beginning and end of study. The results showed four weeks of LIM and LIM + MHY1485 induced a significant degree of myopia shift, compared to the negative control (Control, -2.04 ± 0.60; LIM −6.21 ± 0.55; LIM + MHY1485, -9.14 ± 1.11, diopters, $P<0.0001$). The cross-sectional SS-OCT showed clear boundaries of the inner and outer boundaries of the sclera. At baseline, the mean sclera thickness was 105.05 ± 5.41 µm. At the end of the study, sclera thickness significantly correlated with axial length (coefficient = -4.49 µm for every 0.1 mm axial length increase, 95%CI: -3.56 to -5.83 µm, $P<0.001$) and refractive error (coefficient = -2.77 µm for every 1 diopter myopic shift, 95%CI: -2.06 to -3.47 µm, $P<0.001$) among all guinea pigs. Sclera thickness also significantly correlates with choroidal thickness and choroidal vascularity index (%). In conclusion, the present study shows SS-OCT can be used as a non-invasive method to evaluate sclera thickness and monitor myopia progression in the guinea pig model of LIM.

Keywords Myopia, Sclera thickness, Guinea pigs, Optical coherence tomography

Introduction

Myopia has become one of the most common causes of vision impairment in the general population [1]. Excessive axial elongation during myopia progression can lead to high myopia and retina pathologies, causing irreversible loss of vision and blindness [2]. It was estimated that 5.2% of the global population had high myopia in 2020, which will increase to 9.8% by 2050 [3]. Myopia can be corrected with glasses, contact lenses, or refractive surgery to obtain desirable visual acuity. Several interventions have been shown to be effective in preventing myopia onset and progression, including increasing outdoor activity, low concentration of atropine, and

†Ruiheng Zhang and Chuyao Yu contributed equally to this work.

*Correspondence:
Wenbin Wei
weiwenbintr@163.com
[1]Beijing Key Laboratory of Intraocular Tumor Diagnosis and Treatment, Beijing Tongren Hospital, Beijing Tongren Eye Center, Capital Medical University, 1st Dong Jiao Min Lane, Beijing, China
[2]Beijing Ophthalmology & Visual Sciences Key Lab, Beijing Tongren Hospital, Capital Medical University, Beijing, China
[3]Medical Artificial Intelligence Research and Verification Key Laboratory of the Ministry of Industry and Information Technology, Beijing Tongren Hospital, Capital Medical University, Beijing, China

orthokeratology lenses [1]. However, the mechanism underlying axial elongation and development of myopic maculopathy is still unknown. Thus, exploring the mechanism of myopia progression becomes a research priority for preventing high myopia and its related irreversible vision loss [4].

Guinea pigs are widely used as a animal model of experimental myopia. By placing negative lenses or performing form-deprivation to guinea pig's eye, the guinea pigs developed axial eye elongation and a significant degree of myopia [5]. Thus, the guinea pigs model of lens-induced myopia (LIM) is widely used to explore the mechanism of myopia development and progression [6, 7]. Under negative lenses induction or form-deprivation, the guinea pig' eyes undergo sclera remodeling, which includes collagen fiber destruction, disorganization, and eventually sclera thinning [8]. Recently, it was also used to evaluate the efficiency and safety of myopia interventions, such as posterior scleral reinforcement surgery [9, 10]. By enhancing scleral biomechanical strength through sclera cross-linking, several researchers have found that the scleral reinforcement strategy can be a novel intervention for myopia control [9, 10]. Thus, in-vivo visualizing the sclera of guinea pigs is important for monitoring the dynamic changes of the sclera remodeling in experimental myopia [11].

In the previous study, our team found that combining overactivation of mechanistic target of rapamycin complex 1 (mTORC1) by intravitreal injecting its agonist MHY1485 and placing negative lens defocus could induce high myopia fundus changes in guinea pigs [7]. mTORC1 is a key regulator for basic physiological and pathophysiological processes, including cell growth, metabolism, and survival [12]. It also coordinates anabolic and catabolic cellular processes with inputs such as growth factors and nutrients. Intravitreal injections of mTORC1 agonist in the guinea pig model of LIM enhanced axial elongation, choroid thinning, and parapapillary choroidal atrophy, which resemble fundus characteristics of high myopia in humans.

Swept-source optical coherence tomography (SS-OCT) is a non-invasive imaging technique to visualize the posterior segment of the eye in humans. In the present study, by using such an animal model, we aim to propose a novel method to visualize the sclera in-vivo by a commercially available SS-OCT device and explore the correlation between axial elongation, choroid thinning, decreased choroidal vascularity index (CVI) and sclera thinning.

Methods

The study design, including the management and care of the animals, was approved and supervised by the Ethics Committee of Beijing Tongren Hospital (TREC2023-KY076). All animal experiments complied with the ARRIVE guidelines and follow the U.K. Animals (Scientific Procedures) Act, 1986, and associated guidelines. The study included male pigmented three-week-old guinea pigs, purchased from Beijing Xinruiya Experimental Animal Breeding Co., Ltd (China), reared in cycles of 12-hour light (450–500 lx) and 12-hour dark (~0 lx) with room temperature maintained at 24 ± 2 °C. All animals had ad libitum access to food and water. Humane euthanasia methods ensured that animals are unconscious and free from pain. In this study, guinea pigs were euthanized via intraperitoneal injection of pentobarbital at a dose of 30 mg/kg, followed by cervical dislocation under deep anesthesia. These methods adhere to ethical standards, prioritizing the welfare and dignity of the animals throughout the entire process.

Animal and negative lens-induced myopia (LIM)

Three-week-old tricolor guinea pigs were used in the current study. The guinea pigs were randomly divided into three groups: (1) negative control groups: guinea pigs without LIM ($n = 8$); (2) LIM group: guinea pigs that underwent only monocular LIM ($n = 10$); (3) LIM + MHY1485 group: to induce experimental high myopia, guinea pigs were subjected to monocular LIM and intravitreally injected with a mTORC1 agonist (MHY1485, 4 μg) into the LIM eye once a week for four weeks (at the beginning of the week, $n = 10$).

The details of LIM were described in the previous study [7]. In brief, to induce LIM, goggles fitted with −10.0 diopter lenses (polymethyl methacrylate; diameter: 12.7 mm) were taped onto the orbital rims of both eyes of the guinea pigs. Guinea pigs could open their eyes and blink freely while wearing the goggles. The refractive power of the lens and its centration were measured and verified before application. The lenses were examined daily to ensure they were clean and in place; otherwise, they were detached and replaced with new lenses. The goggles were removed weekly for biometric examinations of the eyes.

Intravitreal injection and high myopia induction

The previous study showed that negative lens induction combined with weekly application of mTORC1 agonist (MHY1485, 4 μg) through intravitreal injections could induce promoted axial elongation, choroid thinning, and peripapillary choroidal atrophy [7]. The preparation of MHY1485 was described previously [7]. MHY1485 (GlpBio Technology, Montclair, CA, USA) is suspended by adding 5% polysorbate 80 (Sigma–Aldrich Co., St. Louis, MO, USA) to phosphate-buffered saline (PBS, Sigma–Aldrich Co.), then immediately aliquoted and stored at -20 °C. The suspensions were thawed and shaken well before use. Intravitreal injections were performed under

topical anesthesia using 0.5% proxymetacaine hydrochloride eye drops (Alcon, Japan). A 26-gauge needle (0.26 mm inner diameter) was used as a trocar needle to make a vitreous entry port 2 mm posterior to the limbus. A 32-gauge Hamilton microsyringe (outer diameter: 0.235 mm, Hamilton Microliter syringe, Sigma–Aldrich Co.) delivered 5 µL of the suspensions into the eyes through the 26-gauge trocar needle. The guinea pigs in the negative control group and LIM group also received 5 µL of PBS with 5% polysorbate 80 once a week in the right eye.

Choroidal thickness, CVI, and sclera thickness measurement

All guinea pigs underwent SS-OCT imaging (VG200D, SVision Imaging, Ltd., Guangdong, China) at baseline and the end of the study, which operated at 200,000 Hz at a 1050 nm wavelength. Because of the potential effect of anesthesia on choroid blood flow, all OCT imaging were performed without anesthesia. Guinea pigs gently maintained a horizontal position, with the superior line of the eyeball parallel to the vertical scan line (Fig. 1A). Then, the OCT scans were performed using a star scan pattern centered on the optic disc center. The horizontal and vertical scan images were selected. For each guinea pig, the choroidal and sclera thickness was measured at the horizontal (3 o'clock and 9 o'clock positions) and vertical meridians (12 o'clock and 6 o'clock positions), three-disc diameters (DD) away from the optic disc center (Fig. 1B). The mean choroidal and sclera thickness was calculated as the average of the four measurement points. Because Axial scaling is independent of ocular magnification in SS-OCT images [13], the measurement line were maked perpendicular to the wall of the retina. (Fig. 1C)

To analyze choroidal vascularity index (CVI), the SS-OCT horizontal and vertical images were selected and converted to a binary image using ImageJ software (ImageJ, U. S. National Institutes of Health, Maryland, USA). Then, the area of interest of the choroid is manually selecting the area within the choroid-RPE junction,

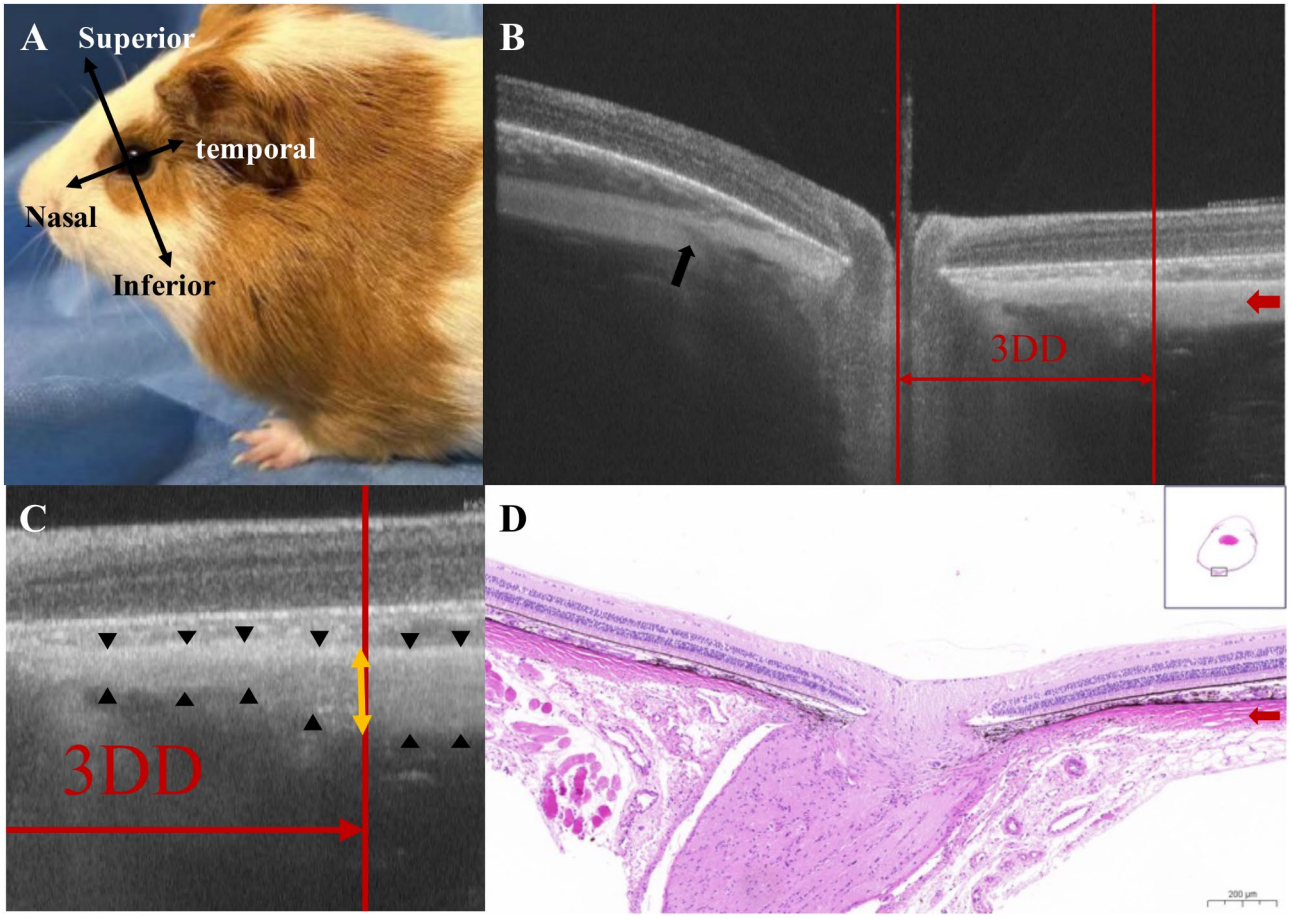

Fig. 1 Demonstration of in-vivo sclera thickness measurement by cross-sectional OCT imaging. (**A**) Near-infrared images of guinea pigs; (**B-C**) OCT images demonstrate designated points to measure sclera thickness; red arrow shows sclera and black arrowheads show the inner and outer boundaries of the sclera. Black arrow: perforating scleral vessels; Red arrow: sclera (**D**) Hematoxylin-eosin staining showed only loose connective tissue beneath the sclera, which justify the selection of sudden drop-off in signal on SS-OCT is posterior scleral boundary

the inner boundary of the sclera, and the vertical line that three disc diameters away from the optic disc center, using the polygon selection tool. Brightness and contrast were adjusted to visualize the choroidal vessels clearly and also to minimize the noise in the OCT images. The Niblack's auto local threshold technique was applied to distinguish luminal area from choroidal area. Then, CVI was calculated as the ratio of luminal area to choroidal area, presented as a percentage.

Biometric measurements

All guinea pigs weekly underwent A-scan ultrasonography and retinoscopy, before intravitreal injections. Under topical anesthesia (0.5% proxymetacaine hydrochloride, Alcon, Japan), we measured the axial length, anterior chamber depth, lens thickness, and vitreous chamber thickness by ocular ultrasound (A-scan mode scan; oscillator frequency: 11 MHz; Quantel Co., Les Ulis, France). The ultrasound velocities used were 1,557.5 m/s for the cornea and aqueous humor, 1,723.3 m/s for the lens, and 1,540 m/s for the vitreous cavity [14, 15]. According to the previous study, the standard deviation of repeated measurement of axial length is 0.056 mm by A-scan ultrasonography [16]. Thus, five measurements were performed for each guinea pig, and the mean values were recorded. The axial length measured by A-scan ultrasonography represents the distance from the front of the cornea apex to the internal limiting membrane. Because of the low resolution of the A-scan ultrasonography, it cannot differentiate the anterior chamber from the cornea. Thus, the anterior chamber thickness measurement contains the corneal thickness.

The eye's refractive status was examined using a streak retinoscope (66 Vision Tech, Suzhou, China) and trial lenses in a dark room. Cycloplegia was achieved with three drops of 1% Mydrin P (Tropicamide 0.5%, phenylephrine HCl 0.5%, Santen Pharmaceutical, Japan) with a 5 min interval before retinoscopy. Refractive errors of the horizontal, vertical, and meridians were measured three times, and the means of refractive measurements were recorded. During the refractive status examination, a small eye would lead to a retinoscopic artifact. This is caused by the fact that the retinal layer that reflects the retinoscopic light is situated within the vitreous-retina interface, rather than the photoreceptors. To eliminate retinoscopic artifacts, the formula was used as follows: Refractive (actual) = Refractive (measured)- $N_V \times T_{retina}/P' \times AL \times (AL - T_{retina})$. The values of refractive index of vitreous chamber (N_V) and posterior focal length divided by axial length (P') were 1.336 and 0.75, respectively [14]. The value of the thickness of the retina (T_{retina}) was 0.13×10^{-3} m from guinea pigs at 4 weeks of age, and the axial length (AL) was individual eye data that was measured by A-scan ultrasonography at the time of retinoscopy.

Streak retinoscopy and A-scan ultrasound was measured by before intravitreal injections. Refractive media occupation, including cataract and vitreous opacities were also identified by retinoscopy. The present study excluded guinea pigs with media occupation.

Statistical analysis

Statistical analyses were conducted using the Stata 17.0 software program (StataCorp, College Station, TX, USA) and GraphPad Prism 9.3.1 (GraphPad Software, San Diego, CA, USA). Unless stated otherwise, continuous variables are presented as the mean ± standard deviation. Comparisons of multiple measurements from the same set of animals at different time points were performed by applying repeated-measures ANOVA (analysis of variance) and then using a Tukey HSD (Honestly Significant Difference) post hoc analysis to identify which differences between pairs of means were significant. To evaluate inter-observer difference, two authors (RHZ and CYY) were asked to measure sclera thickness independently. A Bland-Altman analysis was performed to assess interobserver consistency. P values < 0.05 were considered to indicate statistical significance.

Results

Biometric measurements of LIM and MHY1485-induced high myopia

After four weeks of negative lens induction, the LIM group guinea pigs showed a significant increase in axial length compared to the negative control group. These were two guinea pigs in LIM and LIM + MHY1485 groups were excluded because of cataract and vitreous opacities. Combining intravitreal MHY1485 injections and LIM further enhanced axial elongation (Control, 8.50 ± 0.03 mm; LIM 8.735 ± 0.05 mm; LIM + MHY1485, 8.92 ± 0.06 mm, F (8, 87) = 53.26, P < 0.0001, Fig. 2A). After correcting for retinoscopic artifacts, all guinea pig eyes were near emmetropic at baseline. After four weeks of negative lens induction, guinea pigs showed significant myopic shift compared to negative control eyes. Similarly, after applying intravitreal MHY1485 in eyes received LIM, the degree of myopia was much more significant than LIM alone (Control, -2.04 ± 0.60 D; LIM − 6.21 ± 0.55 D; LIM + MHY1485, -9.14 ± 1.11 D, F (8, 87) = 42.36, P < 0.0001, Fig. 2B). We further analyzed ocular compartment changes during LIM. As exhibited in Fig. 2C-E, axial elongation was primarily due to changes in the depth of the vitreous chamber, followed by lens thickness. In contrast, the cornea and anterior chamber thickness showed no significant changes.

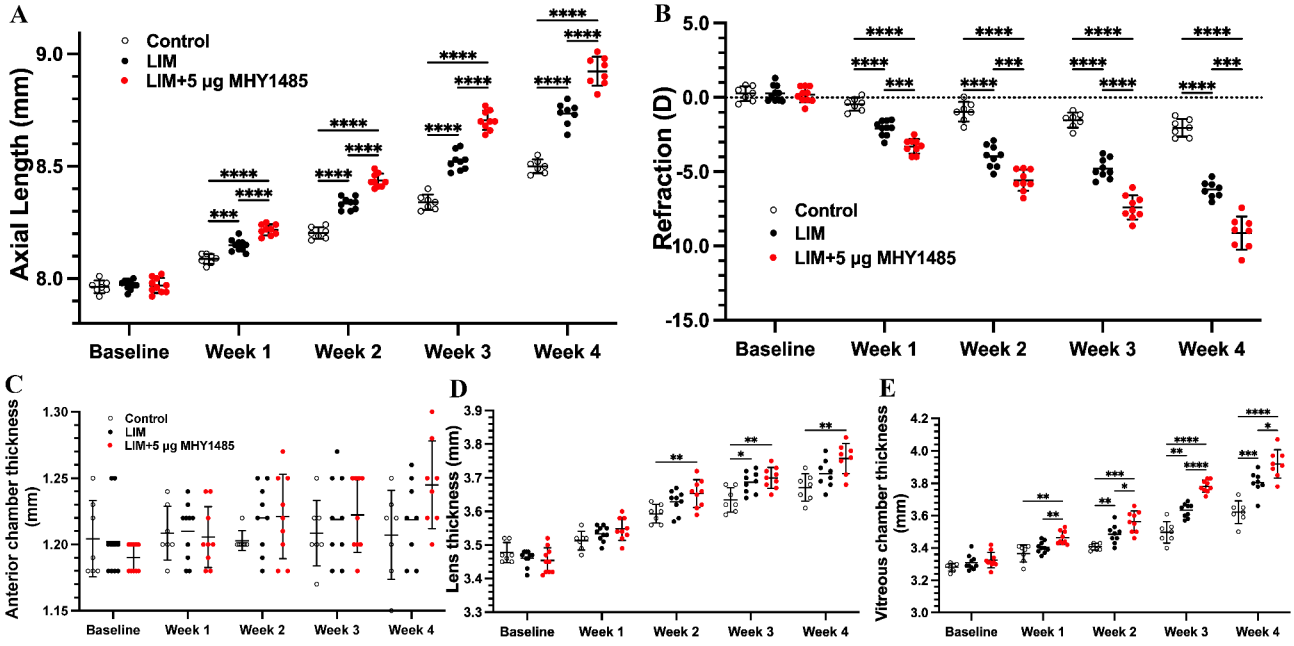

Fig. 2 Axial length, refractive error, and ocular component changes in guinea pigs. The changes in axial length (**A**), refractive error (**B**), anterior chamber depth (**C**), lens thickness (**D**), and vitreous chamber thickness (**E**) were measured. * $P<0.05$, ** $P<0.01$, *** $P<0.001$, **** $P<0.0001$

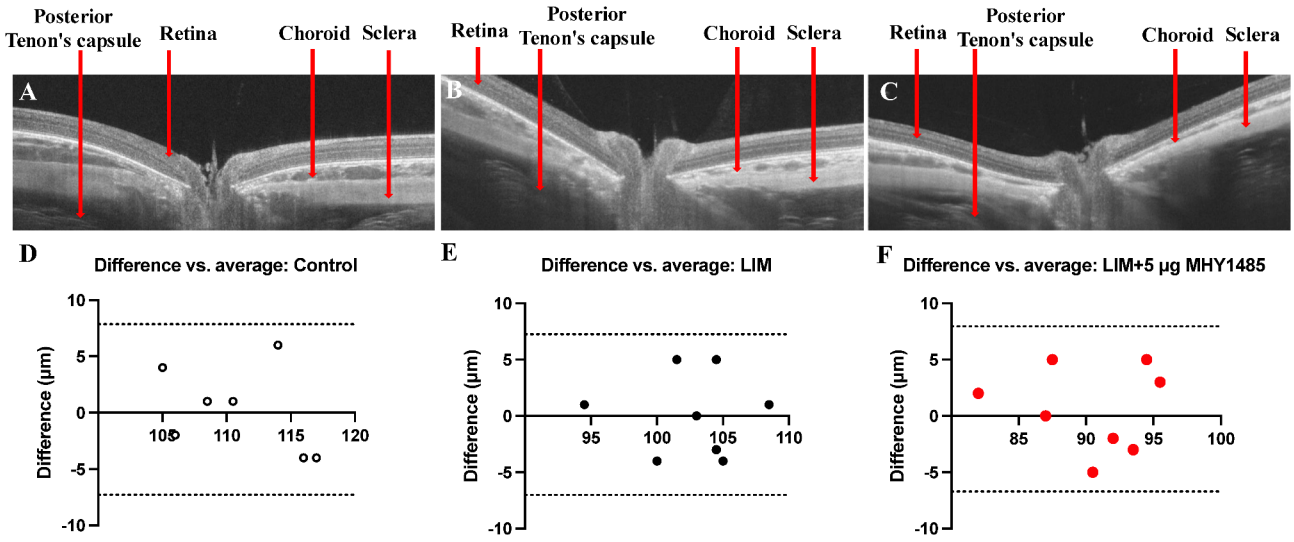

Fig. 3 Represent images, and Bland-Altman analysis showing the inter-observer repeatability for measurements of the sclera thickness. Representative cross-sectional images of the eye with normal control (**A**), negative lens-induced myopia (**B**), and combining monocular LIM and intravitreally mTORC1 agonist (**C**). Bland-Altman plots of guinea pigs in normal control (**D**), negative lens-induced myopia (**E**), and combining monocular LIM and intravitreally mTORC1 agonist (**F**). Every dot represents measurement difference between two observers

Sclera thickness measurement

Representative images of negative control, LIM, and LIM + MHY1485 groups were exhibited in Fig. 3. The cross-sectional SS-OCT showed clear boundaries among the retina, choroid, sclera, and posterior Tenon's capsule space. The assessment of the inter-observer reproducibility revealed a high agreement between two independent examiners in measuring sclera thickness. The Bland-Altman plots showed that the 95% limits of agreements in three groups were − 7.28 to 7.85, -7.01 to 7.26, and − 6.70 to 7.95, respectively (Fig. 3).

Correlations between axial length, refractive error, and sclera thickness

The mean sclera thickness at baseline was 105.05 ± 5.41 (μm). No significant difference was found in sclera thickness among negative control, LIM and LIM + MHY1485 groups (Control, 104.01 ± 5.10 μm; LIM 105.88 ± 5.82 μm;

LIM + MHY1485, 105.12 ± 5.82 μm, F (2, 20) = 0.21, P = 0.82, Fig. 4A). At the end of the study, there was a significant negative correlation between axial length and sclera thickness among all guinea pigs that measured (coefficient = -4.49 μm for every 0.1 mm axial length increase, 95%CI: -3.56 to -5.83 μm, P < 0.001, Fig. 4B). Similarly, there was a significant correlation between refractive error and sclera thickness that was measured at the end of the study (coefficient = -2.77 μm for every 1 diopter myopic shift, 95%CI: -2.06 to -3.47 μm, P < 0.001, Fig. 4C).

Correlations between choroidal thickness, choroid blood perfusion, and sclera thickness

We first extracted the CVI in cross-sectional OCT scans (Fig. 5A-B). At the end of the study, there was a significant positive correlation between choroidal thickness and sclera thickness among all guinea

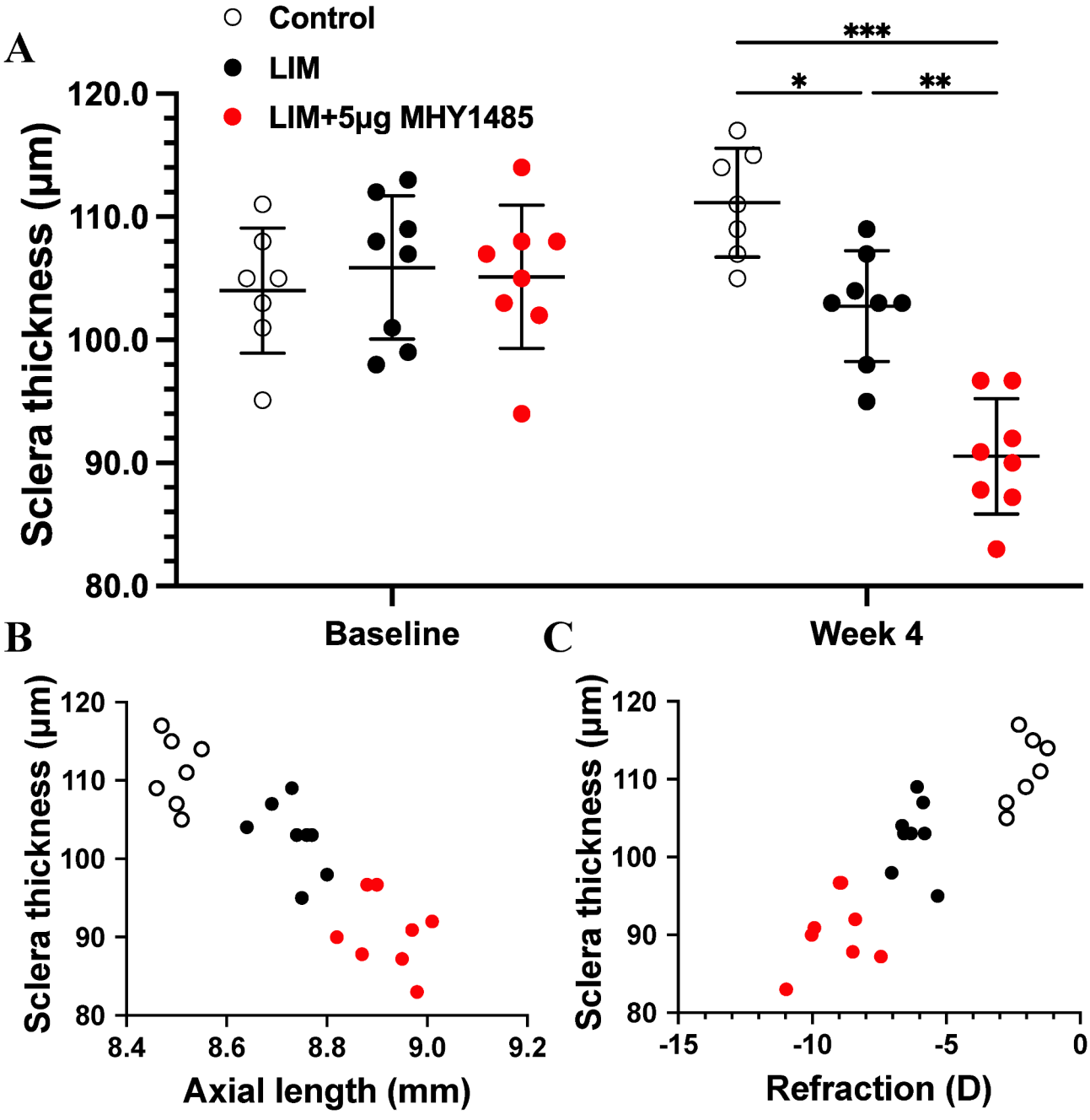

Fig. 4 Correlations between axial length, refractive error, and sclera thickness. * P < 0.05, ** P < 0.01, *** P < 0.001, **** P < 0.0001. (**A**) sclera thickness at baseline and the end of the study. (**B-C**) Two-way scatter plots between axial length, refractive error, and sclera thickness that measured at the end of the study

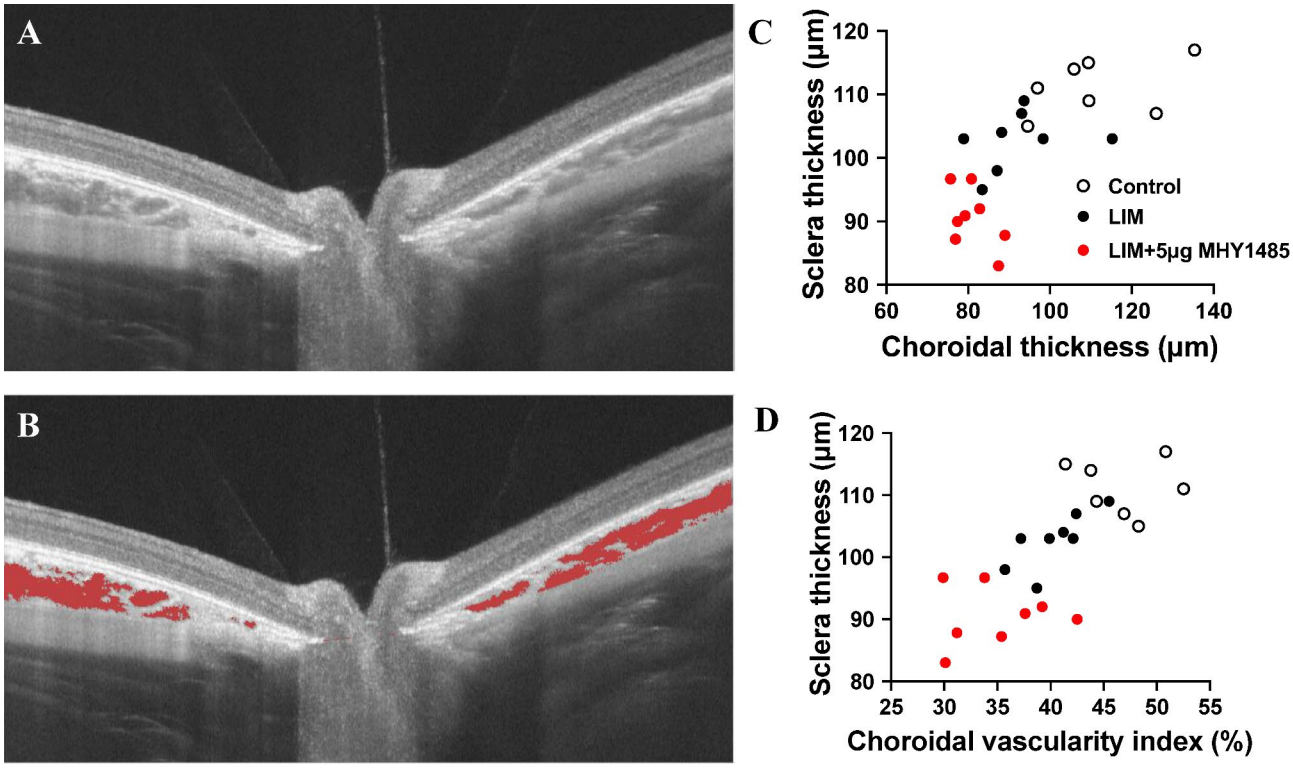

Fig. 5 The correlation between choroidal thickness, blood perfusion, and sclera thickness. (**A-B**) Demonstration of choroidal vascularity index (%) extraction. (**C-D**) Two-way scatter plots between choroidal thickness, choroidal vascularity index (%), and sclera thickness that measured at the end of the study

pigs (coefficient = 1.20 μm for every 1 μm axial length increase, 95%CI: 0.67 to 1.74 μm, $P < 0.001$, Fig. 5C). The sclera thickness was also closely correlated with CVI (%) (coefficient = 0.49% for every 1 μm sclera thickness increase, 95%CI: 0.30 to 0.68 μm, $P < 0.001$, Fig. 5D).

Discussion

In the present study, we found that cross-sectional SS-OCT images exhibited clear boundaries between the retina, choroid, sclera, and posterior Tenon's capsule space. After negative-lens induction, the sclera was progressively thinning, in accordance with axial elongation, myopic shift, choroid thinning, and CVI reduction. The present study reveals that SS-OCT could be a non-invasive method to evaluate sclera thickness in experimental myopia of guinea pigs.

Hyperopic defocus by negative lens-wear is a well-established method for inducing experimental myopia, with the hypothesis that excess axial elongation compensate the hyperopic defocus imposed by the lens [17]. In our pervious study, we found that mTORC1 signaling pathway regulated negative lens induced axial elongation. Intravitreal injection of mTORC1 inhibitor significantly attenuated negative lens induced axial elongation in guinea pigs. The regulative effect of mTORC1 in experimental myopia is seems dependent on abnormal visual input, i.e. hyperopic defocus. In our previous study, weekly injection of 10 μg everolimus into the vitreous body in guinea pigs without negative lens induction did not affect axial length or the fundus appearance [7]. In contrast, intravitreal injection of mTORC1 agonist (MHY1485) significantly promoted axial elongation and choroidal thinning in eyes with negative lens induction [7]. The present study further validated that mTORC1 agonist accelerated myopic shifting, decrease of CVI, and scleral thinning. The underlying mechanism of mTORC1 agonist warrants further investigation.

The sclera is the target organ of myopia progression. Several studies used formalin-fixed paraffin-embedded to measure sclera thickness [18]. This process causes tissue shrinkage due to dehydration, leading to measurement errors [19]. Our previous study showed that OCT-measured retinal and choroidal thickness in guinea pigs is feasible with acceptable inter-observer repeatability and reproducibility. However, the histologic measurements were significantly smaller than OCT by 20.7% and 32.8%, respectively [20]. The current study also showed that SS-OCT-based sclera thickness measurement has a high agreement in inter-observer reproducibility. Considering guinea pigs lack macula structure in their retina, it is challenging for A-scan ultrasonography and optical biometry to locate the exact posterior point of the eyeball. By observing sclera thinning in vivo, SS-OCT could

provide additional parameter to monitor myopia onset and progression in experimental myopia of guinea pigs.

In previous human eye studies and clinical observations, there have been instances where distinguishing between the episclera and Tenon's capsule was challenging [21]. Due to the thinner choroid and sclera compared to human eyes, we found that the inner and outer sclera boundaries and perforating scleral vessels could be easily distinguished in guinea pigs (Fig. 1). Furthermore, lateral magnification can impact the actual location of the measurement points and lead to measurement error when measuring sclera thickness. Commercially available SS-OCT devices are designed with a human schematic eye model and thus cannot be used directly on guinea pigs. Although axial scaling is independent of ocular magnification, a cosine error can also be induced when measuring lines not aligned with OCT scan lines [13]. To avoid this error, the measurement lines should align with the line connecting measurement points and the posterior nodal point. Considering the posterior nodal distance is nearly one-half of the axial length, the back nodal point is located at the approximate center of the eyeball [22]. Thus, we put the measurement line perpendicular to the wall of the retina (Fig. 1).

Sclera thinning and weakening underlie axial elongation during myopia development [23]. In the guinea pig model of LIM, the thickness of the sclera at the posterior pole and the midpoint between the equator and posterior pole decreased significantly with longer axial length [24]. In contrast to measurement based on histologic slides, the present study showed that SS-OCT can be in-vivo and non-invasive in evaluating myopia progression in the guinea pig model of LIM. We further demonstrated that the sclera thinning is closely related to choroid thinning and decreased choroidal blood flow. However, it is still unclear whether there is a causal relationship between choroid thinning and sclera thinning. Several hypotheses have been proposed to explain the observed relationship between choroid thinning and sclera thinning, such as the downregulation of the extracellular matrix components during sclera hypoxia [25, 26]. The sclera stroma mostly lacks capillaries to receive nutrients and oxygen, which requires choroidal blood supplies. The axial elongation-associated choroid thinning may lead to an insufficient oxygen supply to the sclera. After cultivating human scleral fibroblasts in the hypoxia environment (5% oxygen), the expression of collagen-1 was significantly downregulated, suggesting hypoxia may reduce scleral collagen synthesis [26]. Furthermore, the anti-hypoxia drugs salidroside and formononetin ameliorated form deprivation-induced axial elongation in mice, and scleral HIF-1α knockdown led to hyperopia in mice [25, 26]. These results indicated that scleral hypoxia may reduce scleral collagen synthesis, thereby promoting axial elongation.

The limitations of our study should be considered. First, no comparative histology data constitutes the major limitation of the present study. Due to tissue shrinkage during staining, the thickness measured by H&E staining cannot be directly compared to thickness measured by SS-OCT. The use of cryosection is needed to validate the finding of present study. Second, guinea pigs of the control group did not wear plano (0.0 diopter) lenses, so some of the LIM effects may in fact have been accidental form-deprivation effects. Third, The guinea pigs lack macula structure and retinal vessels, making it challenging to locate the same position for different guinea pigs. We maintained a level head position during measurement, and used the average of the four measurement points to minimize position error. Fourth, the lateral magnification is difficult to evaluate because these lack a schematic eye of myopic guinea pigs. Thus, we used an alternative method that measures sclera thickness at three disc diameters away from the optic disc center, resulting in more peripheral measurement points in smaller eyes. Fifth, the present study only carried out SS-OCT measurements for 4-week duration. Future studies are needed for longitudinal examinations.

Conclusion

In conclusion, the present study shows SS-OCT can be used as a non-invasive method to evaluate sclera thickness and monitor myopia progression in the guinea pig model of LIM.

Supplementary Information

The online version contains supplementary material available at https://doi.org/10.1186/s12886-025-03936-w.

Supplementary Material 1

Acknowledgements

None.

Author contributions

R.Z. and C.Y. designed the structure of the manuscript and wrote the manuscript. L.D., H.L., X.S., H.W., Y.L. and W.Z. help collect the data. W.W. revisied the manuscript. All the authors participated in planning, execution, and analysis and have read and approved the final submitted version.

Funding

This study was supported by the National Natural Science Foundation of China (82220108017, 82141128, 82401283); The Capital Health Research and Development of Special (2024-1-2052); Science & Technology Project of Beijing Municipal Science & Technology Commission (Z201100005520045);Sanming Project of Medicine in Shenzhen (No. SZSM202311018); R&D Program of Beijing Municipal Education Commission (No. KM202410025011); The priming scientific research foundation for the junior researcher in Beijing Tongren Hospital, Capital Medical University (No. 2023-YJJ-ZZL-003).

Data availability
All data included in this study are available upon request by contact with corresponding author.

Declarations

Ethics approval and consent to participate
The experimental protocol was approved by the Ethics Committee of Beijing Tongren Hospital (TREC2023-KY076). All animal experiments complied with the ARRIVE guidelines and follow the U.K. Animals (Scientific Procedures) Act, 1986, and associated guidelines.

Consent for publication
Not applicable.

Competing interests
The authors declare no competing interests.

Received: 31 October 2024 / Accepted: 18 February 2025
Published online: 03 March 2025

References

1. Baird PN, Saw SM, Lanca C, Guggenheim JA, Smith Iii EL, Zhou X, Matsui KO, Wu PC, Sankaridurg P, Chia A et al. Myopia. Nat Rev Dis Primers 2020;6(1):99.
2. Tang Y, Wang X, Wang J, Huang W, Gao Y, Luo Y, Lu Y. Prevalence and causes of visual impairment in a Chinese adult population: the Taizhou eye study. Ophthalmology. 2015;122(7):1480–8.
3. Wong TY, Ferreira A, Hughes R, Carter G, Mitchell P. Epidemiology and disease burden of pathologic myopia and myopic choroidal neovascularization: an evidence-based systematic review. Am J Ophthalmol 2014, 157(1).
4. Morgan IG, French AN, Ashby RS, Guo X, Ding X, He M, Rose KA. The epidemics of myopia: aetiology and prevention. Prog Retin Eye Res. 2018;62:134–49.
5. Dong L, Shi XH, Kang YK, Wei WB, Wang YX, Xu XL, Gao F, Yuan LH, Zhen J, Jiang WJ, et al. Amphiregulin and ocular axial length. Acta Ophthalmol. 2019;97(3):e460–70.
6. Dong L, Shi XH, Li YF, Jiang X, Wang YX, Lan YJ, Wu HT, Jonas JB, Wei WB. Blockade of epidermal growth factor and its receptor and axial elongation in experimental myopia. FASEB J. 2020;34(10):13654–70.
7. Zhang R, Dong L, Wu H, Shi X, Zhou W, Li H, Li Y, Yu C, Li Y, Nie Y, et al. mTORC1 signaling and negative Lens-Induced axial elongation. Invest Ophthalmol Vis Sci. 2023;64(10):24.
8. Harper AR, Summers JA. The dynamic sclera: extracellular matrix remodeling in normal ocular growth and myopia development. Exp Eye Res. 2015;133:100–11.
9. Lai L, Lv X, Wu X, Xu Y, Chen Z, Li Y, Sun M, Zhang F. Comparing the differences in slowing myopia progression by riboflavin/ultraviolet A scleral Cross-linking before and after Lens-induced myopia in Guinea pigs. Curr Eye Res. 2022;47(4):531–9.
10. Guo L, Hua R, Zhang X, Yan TY, Tong Y, Zhao X, Chen SC, Wang M, Bressler NM, Kong J. Scleral Cross-Linking in Form-Deprivation myopic Guinea pig eyes leads to glaucomatous changes. Invest Ophthalmol Vis Sci. 2022;63(5):24.
11. Liu X, Jiang L, Ke M, Sigal IA, Chua J, Hoang QV, Chia AWI, Najjar RP, Tan B, Cheong J, et al. Posterior scleral birefringence measured by triple-input polarization-sensitive imaging as a biomarker of myopia progression. Nat Biomedical Eng. 2023;7(8):986–1000.
12. Saxton RA, Sabatini DM. mTOR signaling in growth, metabolism, and disease. Cell. 2017;168(6):960–76.
13. Salmon AE, Sajdak BS, Atry F, Carroll J. Axial scaling is independent of ocular magnification in OCT images. Invest Ophthalmol Vis Sci. 2018;59(7):3037–40.
14. Zhou X, Qu J, Xie R, Wang R, Jiang L, Zhao H, Wen J, Lu F. Normal development of refractive state and ocular dimensions in guinea pigs. Vis Res. 2006;46(18):2815–23.
15. Norton TT, McBrien NA. Normal development of refractive state and ocular component dimensions in the tree shrew (Tupaia belangeri). Vis Res. 1992;32(5):833–42.
16. Wang Q, Ji X, Lu D, Zhu Y, Whelchel A, Wang J, Zhang H, Dong L, Wei R. Comparison of A-Scan ultrasonography and the lenstar optical biometer in Guinea pig eyes. Exp Eye Res. 2021;207:108578.
17. Morgan IG, Ashby RS, Nickla DL. Form deprivation and lens-induced myopia: are they different? Ophthalmic Physiol Opt. 2013;33(3):355–61.
18. Zi Y, Deng Y, Zhao J, Ji M, Qin Y, Deng T, Jin M. Morphologic and biochemical changes in the retina and sclera induced by form deprivation high myopia in guinea pigs. BMC Ophthalmol. 2020;20(1):105.
19. Turunen MJ, Khayyeri H, Guizar-Sicairos M, Isaksson H. Effects of tissue fixation and dehydration on tendon collagen nanostructure. J Struct Biol. 2017;199(3):209–15.
20. Dong L, Li YF, Jiang X, Lan YJ, Shao L, Jonas JB, Wei WB. In vivo imaging of retina and choroid in Guinea pigs. Front Med (Lausanne). 2021;8:730494.
21. Ohno-Matsui K, Fang Y, Morohoshi K, Jonas JB. Optical coherence tomographic imaging of posterior episclera and Tenon's capsule. Invest Ophthalmol Vis Sci. 2017;58(9):3389–94.
22. Howlett MHC, McFadden SA. Emmetropization and schematic eye models in developing pigmented guinea pigs. Vis Res. 2007;47(9):1178–90.
23. Vurgese S, Panda-Jonas S, Jonas JB. Scleral thickness in human eyes. PLoS ONE. 2012;7(1):e29692.
24. Dong L, Shi XH, Kang YK, Wei WB, Wang YX, Xu XL, Gao F, Jonas JB. Bruch's membrane thickness and retinal pigment epithelium cell density in experimental axial elongation. Sci Rep. 2019;9(1):6621.
25. Zhao F, Zhang D, Zhou Q, Zhao F, He M, Yang Z, Su Y, Zhai Y, Yan J, Zhang G, et al. Scleral HIF-1α is a prominent regulatory candidate for genetic and environmental interactions in human myopia pathogenesis. EBioMedicine. 2020;57:102878.
26. Wu H, Chen W, Zhao F, Zhou Q, Reinach PS, Deng L, Ma L, Luo S, Srinivasalu N, Pan M, et al. Scleral hypoxia is a target for myopia control. Proc Natl Acad Sci U S A. 2018;115(30):E7091–100.

Publisher's note